VOLUME 5, NUMBER 3, MARCH 2005

NANO LETTERS

Confined Phonons in Si Nanowires

K. W. Adu,[†] H. R. Gutiérrez,[†] U. J. Kim,[†] G. U. Sumanasekera,[‡] and P. C. Eklund*[,†,§]

Department of Physics, The Pennsylvania State University, University Park, Pennsylvania 16802, Department of Physics, 102 Natural Sciences Bldg., University of Louisville, Louisville, Kentucky 40292, and Department of Materials Science, The Pennsylvania State University, University Park, Pennsylvania 16802

Received August 24, 2004; Revised Manuscript Received December 14, 2004

ABSTRACT

Raman microprobe studies of long crystalline Si nanowires reveal for the first time the evolution of phonon confinement with wire diameter. The Raman band at ~520 cm^{-1} in bulk Si is found to downshift and asymmetrically broaden to lower frequency with decreasing wire diameter $\bar{D}$, in good agreement with a phenomenological model first proposed by Richter et al. An adjustable parameter (α) is added to the theory that defines the width of the Gaussian phonon confinement function. We find that this parameter is not sensitive to diameter over the range 4–25 nm.

Several Raman scattering studies of long wavelength phonons in crystalline Si nanowires have appeared in the literature over the past several years.[1−7] The authors have fitted the first-order experimental Raman band near 520 cm^{-1} to an asymmetric line shape first proposed by Richter et al.[8] In this model, the confined phonon participating in the Raman scattering event is expressed as a wave packet using bulk phonon states. The range of bulk wavevector δq needed to form the packet is given by $\delta q \sim 1/D$, where D is the filament diameter. In limit of infinite D, the symmetric Lorentzian line shape representing the first order scattering from the degenerate LO−TO $q = 0$ phonons of bulk Si is recovered from the model expressions. None of the previous experimental studies have looked systematically at the effect of the wire diameter on the Raman line shape, i.e., the effects of the most important physical parameter has not been investigated. Here, we present the results of such a study made on a series of four crystalline Si nanowire samples whose most probable diameter $\bar{D}$ spans the range from $4 \leq \bar{D} \leq 25$ nm. All other optical parameters, e.g., laser flux wavelength and optics, are the same for each Raman spectrum collected; the wire diameter is the only variable. Silicon, as a well-understood elemental semiconductor, is chosen to explore the basic phenomenon of phonon confinement.

Usually there is insufficient signal to study the Raman scattering from a single semiconducting nanowire, and therefore ensembles of nanowires are measured. Since the diameter of the nanowire produces the confinement parameter, it is important to be able to either rule out significant

* Corresponding author. E-mail: pce3@psu.edu.
[†] Department of Physics, PSU.
[‡] University of Louisville.
[§] Department of Materials Science, PSU.

10.1021/nl0486259 CCC: $30.25
Published on Web 01/28/2005

inhomogeneous broadening of the Raman band from the experimental diameter distribution or to include the distribution in the line shape analysis. To date, all of the previous studies of the first-order Raman band in Si nanowires, except one,[7] have used an estimated mean nanowire diameter in their data analysis. We also show here that for quantitative anlaysis the distribution should be included. There also have been other complicating factors slowing progress in understanding the Raman line asymmetry encountered in the first-order band in Si nanowires and other nanosystems, e.g., possible complications from the effects of compressive strain[9] and laser flux-induced changes in the line shape asymmetry.[4−6] For example Piscanec et al.[4,5] argued that the Raman band asymmetry in Si nanowires has a contribution from inhomogeneous laser heating, whereas Gupta et al. presented evidence for a photo/thermal-driven Fano resonance.[6] Adu et al., on the other hand, have found that the SiO_x covering the Si wire can produce a compressive strain on the crystalline core, upshifting the band position but not changing the band asymmetry.[9]

According to a phenomenological theory,[8,10] phonon confinement in a small nanosystem (e.g.,particle, nanowire) leads to an asymmetric broadening of the Raman bands. The theory for this confinement predicts a specific evolution with decreasing diameter D. The effect becomes very important when the diameter of the particle or wire is $d \sim 10a_o$, where a_o is the lattice constant. This report is the first, to our knowledge, to look at the systematics of how the first-order Raman band changes with decreasing diameter.

All experiments were carried out in the same way (exactly the same collection optics) and at very low laser flux (< 10 $\mu W/\mu m^2$). At a factor of 2 or so greater than this flux, we observed the 520 cm^{-1} band line shape changing in small diameter wires. More importantly, we also observed this effect in much larger diameter wires, i.e., those with $\bar{D} \sim$ 23 nm, where no phonon confinement is expected. This indicates that both confinement and unrelated high flux phenomena can occur together. We will present these high flux results elsewhere.[11]

Here, we concentrate on Raman scattering data collected in the region of low laser flux $\Phi \leq 10$ $\mu W/\mu m^2$ where the shape of the 520 cm^{-1} band is independent of Φ. Previously, we have also published results of a Raman study on ~9 nm diameter Si wires that showed growing asymmetry to lower frequency in the ~520 cm^{-1} band with increasing laser flux. A broadened line shape was observed and well fit by a Fano resonance.[6] However, we have revisited that work and we have repeated it for very small and very large diameter Si wires. Our new experimental evidence also suggests that a more likely mechanism for the increased asymmetry in the high flux regime is inhomogeneous laser heating, in agreement with Piscanec et al.[4]

The Si nanowires studied here were prepared by pulsed Nd:YAG laser vaporization (PLV) of a Si target (99.999%, Alfa Aesar) containing ~10 at. % Fe(99.9+%, Aldrich). The target was maintained at 1200 °C in a flow of 100 sccm of argon gas. Details of our synthesis approach have been given elsewhere.[12] Our TEM analysis clearly indicates that the wire growth process occurs via the vapor−liquid−solid (VLS) mechanism[12,13] in which an Fe/Si nanodroplet (liquid alloy) or nanoparticles acting as "seeds" form in the laser-generated plume, adsorb Si vapor, and become Si-saturated. The Si filaments grow from the Fe/Si nanoparticle surface. Our PLV approach tends to make wires with a broad diameter distribution in the 8−40 nm diameter range. To produce smaller diameter wires for this study, we developed a post-synthesis approach involving oxidation in pure O_2 at 900 °C as a first step and centrifugal separation as the second step. The idea is to diffuse oxygen radially inward, shrinking the Si crystalline core, and then to separate fractions according to diameter via centrifugation. Details of this approach to smaller diameter Si (and other semiconducting) wires will appear elsewhere.[9]

The oxidized Si wires were first harvested from a cool furnace and then suspended in ethanol using ultrasound. A centrifugal separation technique was then used to divide the original as-grown wires into four distinct diameter distributions. After short intervals of centrifugation, the centrifuge was stopped, the precipitate was removed, and the supernatant containing smaller diameter wires in solution was saved and centrifuged further; the largest diameter wires and particles are driven from the suspension at the earliest times. Each time, the supernatant fluid was put back into a clean centrifuge tube and spun again. In this way, precipitates were obtained at 5 min (5000 rpm), 10 min (5000 rpm), 40 min (5000 rpm), 70 min (5000 rpm), and 100 min (13500 rpm) of centrifugation. This last step produced the smallest diameter wires, i.e., $\bar{D} = 4.5$ nm. The first precipitate (after 5 min) was found to contain Si particles and therefore was rejected.

High-resolution transmission electron microscopy (HR-TEM) using a JEOL (JEM 2010F) microscope with a 200 kV accelerating voltage was used to observe the nanowires' crystallinity, growth direction, oxide coating, morphology and the Si core diameter distribution. The TEM and Raman samples were prepared by dropping a small amount of the ethanol−nanowire suspension onto either a carbon film-coated Cu grid (TEM) or on indium foil (Raman). The Raman experiments were found to be best conducted by creating a thin, i.e., ≤ 1, monolayer areal density of wires that were in good contact with a thermally conducting substrate (i.e., indium). Raman spectra were collected at room temperature in the backscattering configuration using a JY Horiba T64000 spectrometer equipped with cooled CCD detection and an Olympus BX40 confocal microscope with a 100× objective (spot size at the sample was ~1μ). Excitation was provided by an argon ion laser under ambient conditions using 514.5 nm radiation at a flux of ~8 $\mu W/\mu m^2$, as measured using a miniature hand-held radiometer at the sample. Low excitation power is particularly important, as will be discussed below. No polarizer was used in collecting the backscattered light.

A low resolution TEM image of Si nanowires is shown in Figure 1a. This particular typical image was taken on wires harvested (in the precipitate) from the second centrifugation cycle. This ensemble was found to have a most probable

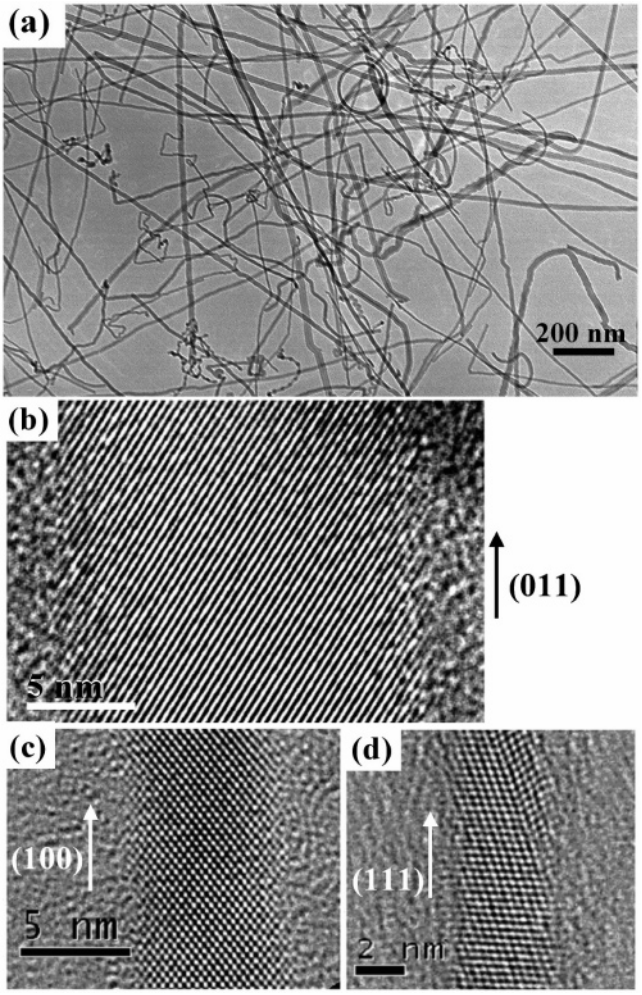

Figure 1. (a) Low magnification TEM showing the Si nanowires ensemble for the sample with 10 min of centrifugation. (b, c, d) High-resolution TEM images of the crystalline core for nanowires with diameter of 16, 7, and 4 nm, respectively.

diameter $\bar{D} = 23$ nm. The image shows that the wires are long (>2 μ), most have long straight sections. However, large angle bends and kinks can be found in some of the wires. After only one cycle of centrifugal separation, the sample was found by TEM to consist primarily of Si wires. In Figure 1b−d, we display HRTEM images of Si nanowires from subsequent centrifuge separations, ranging in diameter from ~16 nm (b) to ~4 nm (d). In general, the Si wires were found to be highly crystalline with a thick 4−10 nm SiO_x coating. The HRTEM images are also included here to make the point that we did not observe a dominant growth direction upon inspection of many wires. As seen in Figure 1b−d, examples can be found for wires growing along the (011), (100), or (111) directions, in contrast to a previous report on Si nanowires grown by CVD with gold nanoparticles,[14] we did not observe any relationship between the wire diameter and growth direction. The growth directions indicated in Figure 1 were determined by correlating the electron diffraction pattern, the Fourier transform of the image, and the lattice fringe spacing.

In Figure 2 we display the diameter distribution (histogram) of the crystalline Si cores in each of the four ensembles studied here; they were obtained by HRTEM. Each distribution was fitted to a log-normal function $F(D)$ (solid line) using the method of least squares; $F(D)$ is given by[15]

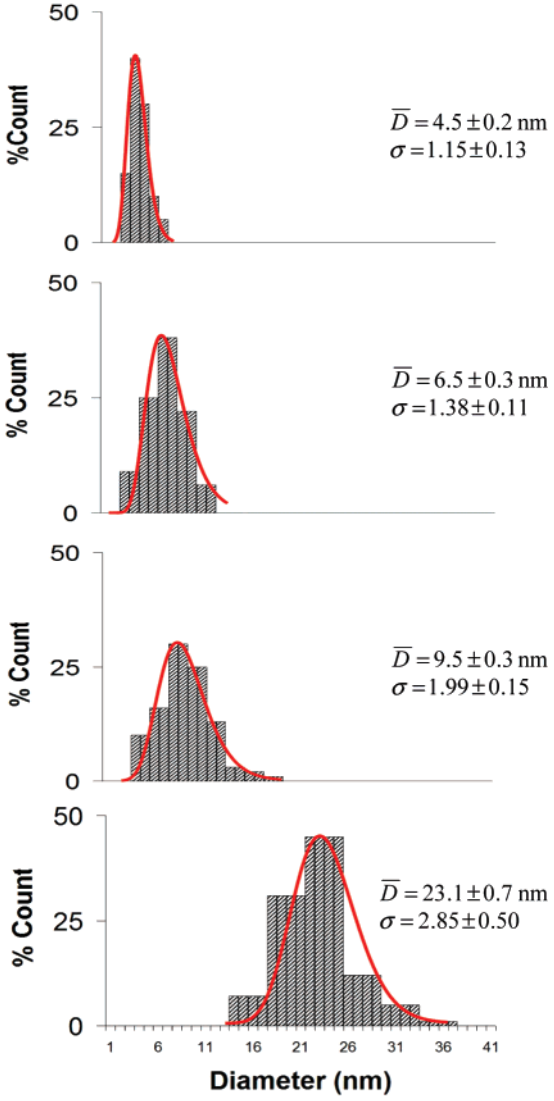

Figure 2. Diameter distributions for the four different samples with the most probable diameters shown in the figure. The distributions were obtained by measuring the crystalline core from HRTEM images of the Si nanowires. The solid lines represent the least-squares fits using the log-normal function $F(D)$ (eq 1).

$$F(D) = \frac{1}{\sigma} \exp - \left[\frac{(\log D - \log \bar{D})^2}{2\sigma^2}\right] \qquad (1)$$

where $\bar{D}$ and σ are, respectively, the most probable value and width of the diameter distribution (the full width at half-maximum (FWHM) is $\sqrt{2}\sigma$). The parameter values for $\bar{D}$,σ obtained from the fits are displayed in the figure along with the computed errors. A log-normal diameter distribution is often found in nanosystems and stems from the relative importance of the surface and volume energies of the wire (or particle).[15,16]

In Figure 3, we display the first-order 520 cm^{-1} Raman bands we obtained at low laser power and at room temperature for the four ensembles of nanowires whose diameter distributions appear in Figure 2. The micro-Raman spectra,

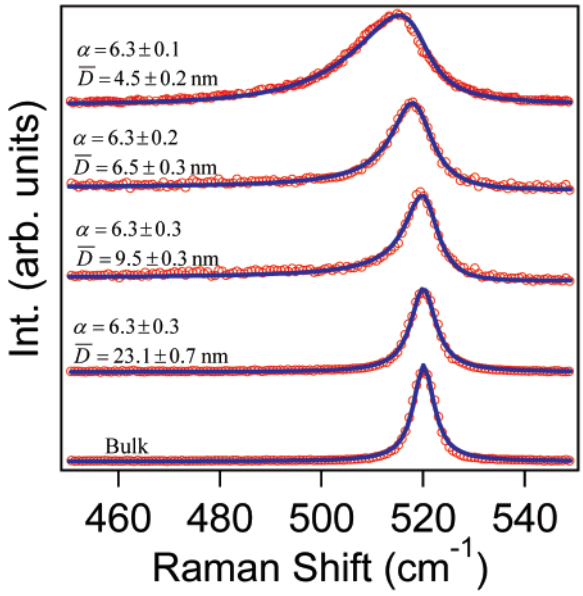

Figure 3. Raman spectra showing the evolution of the first-order Raman band in the four ensembles of Si nanowires of Figure 2. The spectrum corresponding to that of bulk Si (001) is also shown. Open circles represent the experimental data and solid lines represent the least-squares fits using eq 5, in which both the Richter's line shape and the diameter distribution $F(D)$ are taken into account.

all collected under the same optical conditions (see the experimental details section) are stacked in the figure according to most probable diameter $\bar{D}$, with the smallest diameter wire ensemble spectrum on top. For comparison we show the result for bulk Si (001) at the bottom of the figure. The data are represented by open circles and the solid lines are the results from a least squares line shape analysis using the Richter model discussed below. It is clear from Figure 3 that, with decreasing $\bar{D}$, the first-order Raman band at ~520 cm^{-1} develops a noticeable asymmetry to lower frequency and the peak position downshifts. On the other hand, the line shape for bulk Si (bottom band) is well fitted by a symmetric function. The line shape is actually a Voigt function, which is a convolution of a Gaussian spectrometer function (FWHM = 1.5 cm^{-1}) and a Lorentzian (Raman) line shape. The symmetric band we observe for bulk Si at 520 cm^{-1} has a measured FWHM = 4.7 cm^{-1} and a natural FWHM 4 cm^{-1}, in good agreement with the literature.[8,17]

We now analyze the line shape of the asymmetric Raman bands in Figure 3 with the model originally proposed by Richter et al.[8] for spherical particles and extended by Campbell and Fauchet[10] to cylindrical particles. The starting point of their model is to approximate the form of the confined phonon wave function as a simple product of a localization function $W(r,D)$ and the related infinite crystal phonon wave function; the variables r and D are, respectively, the radial coordinate and the physical diameter of the nanoparticle or nanowire. Therefore, the introduction of $W(r,D)$ attenuates the wave function in the confined system near the particle boundary. The confined phonon wave function $\phi(\mathbf{q}_0,\mathbf{r})$ can be written as a superposition of infinite crystal phonon wave functions $\psi(\mathbf{q},\mathbf{r})$, with each $\psi(\mathbf{q},\mathbf{r})$ weighted by the coefficient $C(\mathbf{q}_0,\mathbf{q})$. The $C(\mathbf{q}_0,\mathbf{q})$ are calculated via a Fourier analysis of the localization function $W(r,D)$.[8,10] The Raman line shape for scattering from the confined phonon is then written as the sum of the Raman scattering contributions from $\psi(\mathbf{q},\mathbf{r})$. In our case, we consider the scattering from the 520 cm^{-1} optical mode at $q_o = 0$. The line shape function for scattering from this confined phonon[8,10] in nanowires (NW) is given by

$$I_{NW} = A_o \int_o^{q_{max}} \frac{|C(0,q_\perp)|^2}{[\omega - \omega_o(q_\perp)]^2 + (\Gamma/2)^2} 2\pi q_\perp \, dq_\perp \quad (2)$$

The Raman matrix element $|M_q|$ for scattering from the infinite crystal phonon with frequency $\omega(\mathbf{q})$ is absent in the integrand. This amounts to the approximation that $|M_q|$ is independent of $\mathbf{q}$. $|M_q|^2$ has therefore been factored out of the integrand and appears in front of the integral in the intensity factor A_o. Γ represents the natural FWHM of the bulk Si phonon convoluted with the spectrometer function. To fit our data, we will use $\Gamma = 4.7$ cm^{-1}, which is the value we obtain under identical optical conditions for the FWHM of the bulk Si ~520 cm^{-1} phonon at room temperature. The natural width of this phonon is known to be ~4 cm^{-1} at room temperature.[8,17]

There seems to be a consensus in the literature that a Gaussian form for the confinement envelope function $W(r,D)$ best describes the Raman observations.[2−5,7,8,10,18] However, there seems to be some discussion as to what the exponent should be. Therefore, to be most general, we write W as

$$W(r,D) \sim \exp[-(\alpha r/D)^2] \quad (3)$$

where α is the constant we introduce to be determined by experiment. A wide range of values for α have appeared in the literature.[2−5,7,8,10,18] The value of α, of course, directly impacts the attenuation of the phonon amplitude at the real boundary of the nanosystem, i.e., at $r = D/2$. For example, Richter et al., in their seminal paper on Raman scattering from small Si particles, proposed that $\alpha = 1.4$ provided the best description for their spectra. Campbell and Fauchet, on the other hand, found that a much larger value $\alpha = 8.9$ provided the stronger localization necessary to explain their data on spherical Si and GaAs particles.

For the case of an infinite cylindrical wire, $C(0,q_\perp)$ can be written in terms of α, the nanowire diameter D, and the wavevector transverse to the wire axis $(q_\perp)$[10]

$$|C(0,q_\perp|^2 \sim \exp\left[-\frac{1}{2}\left(\frac{q_\perp D}{\alpha}\right)^2\right] \quad (4)$$

To analyze our Raman data for Si nanowires, we use an isotropic form for the optical phonon dispersion of the bulk Si, i.e., $\omega_o(0,q_\perp) = [A + B\cos(q_\perp a)]^{1/2}$ ($A = 1.714 \times 10^5$ cm^{-2} and $B = 1.0 \times 10^5$ cm^{-2}). A and B were determined from neutron scattering data for the TO branch.[19] In the ideal case, where all wires would grow along the same direction (e.g., (111)), we would use the optical phonon dispersion averaged in a plane perpendicular to the (111) axis. However, we have observed several growth directions in our ensembles (e.g., (111), (100), (011)). Therefore, an isotropic dispersion is a reasonable approximation in our case.

Table 1. Comparison of Different α Values for the Confinement Parameters in the Localization Function $\exp[-(\alpha r/D)^2]$ for Wires and Spherical Particles (c.f., eq (3)) Obtained from the 520 cm^{-1} Raman Band Analysis

α	confinement geometry	material	estimated mean diameter $\bar{D}$ (nm)	ref
8.9	cylinder	Si	10,15,21[b]	3
8.9	sphere, cylinder	nc-Si,[a] Si	10[b]	10
4.4	cylinder	Si	10,15[b]	2(a)
1.4	sphere	nc-Si[a]	10[b]	8
8.9	cylinder	Si	< 20[b]	2(b)
4.4	sphere	nc-Si[a]	2.8−7[b]	18
8.9	cylinder	Si	15[b]	4,5
10.4	cylinder	Si	10[c]	7
4.4	cylinder	Si	60[b]	2(c)
6.3	**cylinder**	**Si**	**4−25[c]**	**present work**

[a] Nanocrystalline material. [b] Line shape calculations use estimated mean diameter. [c] Diameter distribution is used in line shape calculations.

A careful analysis of the line shape must also include the diameter distribution of the nanowire sample.[7] This is done by including in the analysis the log-normal function $F(D)$ that fits the measured diameter distribution in the analysis (cf., Figure 2). That is,

$$I_{NWD}(\omega,\bar{D}) = \int_0^\infty F(D)\, I_{NW}(\omega,D)\, dD \qquad (5)$$

and $I_{NW}(\omega,D)$ is the line shape function for scattering from a single nanowire of diameter D (eq 2). Equation 5 therefore amounts to evaluating a double integral to fit the Raman band; one integral is for the diameter distribution, and the other for the phonon confinement transverse to the wire axis of a specific wire of diameter D.

The results of a nonlinear least-squares fit to the experimental spectra via optimal adjustment of (A_o,α) in eq 5 are shown in Figure 3 as the solid line. As can be seen in the figure, the agreement with experiment is very good. It is important to note that the least squares value for α does not vary much from ensemble to ensemble, whose mean diameters cover a range of $\bar{D}$ = 4.5, 6.5, 9.5, and 23.1 nm. Also, the systematics in the evolution in the line shape data with decreasing wire diameter and the universal value for α extracted from the line shape analyses convince us that kinks or defects in nanowires (c.f., Figure 1a) are not the central issue. This yields the physical result that the scale of the confinement function (α) does not depend on nanowire diameter eq 3. From the quality of the fits, it is clear that the phonon confinement model of Richter et al.[8] describes very well the shape of the ∼520 cm^{-1} Raman bands for our Si nanowire ensembles with diameters down to ∼4 nm. This is somewhat surprising because D = 4 nm is equivalent to only ∼8 lattice constants (α(Si) = 0.543 nm). One might expect that good agreement with experiment might require that the real boundary of the sample be included in a "first principles" lattice dynamics calculation, as has been recently performed by Mahan and co-workers.[20]

In Table 1, we compare our experimental value for α against those we can find in the literature (we computed them according to eq 3). Table 1 shows that a significant range of α has been reported for Si particles and nanowires, i.e., 1.4 < α < 10.4. In support of our value (α = 6.3), we note that

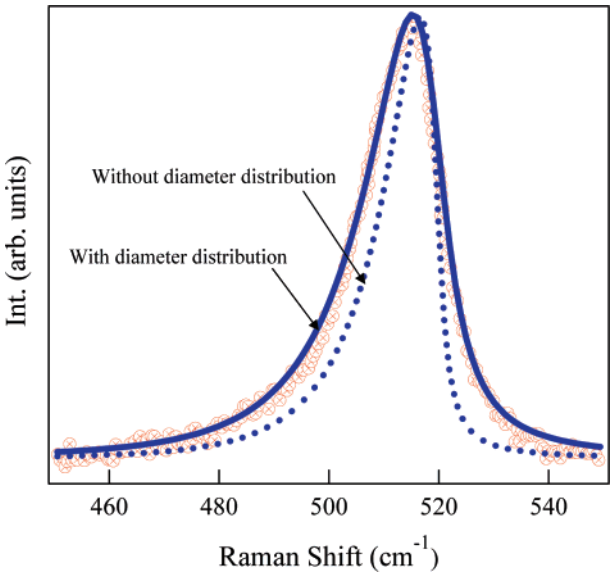

Figure 4. Comparison between the line shape of the first-order Raman band calculated by eq 5 taking into account the diameter distribution (solid line) and by eq 2 without diameter distribution (dashed line). Open circles represent the experimental data for the ensemble with most probable diameter 4.5 nm.

our four Si nanowire samples, which exhibit significantly different diameter distributions, all produce the same value for α = 6.3 ± 0.2. We suspect that the large range of reported experimental values might stem from a variety of unknown conditions, as we alluded to earlier: compressive strain, inhomogeneous laser heating, disordered (less crystalline) material, failure to incorporate the diameter distribution or the proper value for the natural bulk phonon line width (including the spectrometer resolution). However, the nature of the phonon confinement might also be impacted by the thickness and nature of the oxide coating on the wire (even without compressive strain). That is, the phonon in the crystalline core of the nanowire (or nanoparticle) has to decay into phonons in the oxide shell. Therefore, future experiments on hydrogen-terminated Si nanowires should be carried out to see how the hydrogen termination affects the value of the confinement parameter α.

Finally, we would like to make some quantitative remarks about the necessity of including the nanowire diameter distribution in the line shape analysis. If the data were fit with eq 2 using a mean diameter $\bar{D}$ and not integrating over the range of diameter found in the ensemble, one would obtain an artificially enhanced value for α. For example, fitting the four Raman bands in Figure 3 as if each corresponded to a *monodisperse* sample represented by the mean (or most probable) wire diameter, we find α = 7.3 (D = 4.5 nm), α = 7.8 (D = 6.5 nm), α = 8.2 (D = 9.5 nm) and α = 10.9 (D = 23.1 nm). Of course, the error in α made by ignoring the diameter distribution is largest when the diameter distribution is broad. Another way of appreciating the need for including the diameter distribution is to fix α = 6.3 and compute the band shape with, and without, the experimental diameter distribution. This is shown in Figure 4 for the $\bar{D}$ = 4.5 nm sample. As can be seen there, we find that including the diameter distribution increases the apparent FWHM by 30%, a significant increase.

In conclusion, we have found that the phenomenological phonon confinement model of Richter et al. describes very well our experimental Raman line shape for long, small-diameter crystalline Si nanowires. If the measured diameter distribution is taken explicitly into account, we find that an adjustable parameter α introduced to fix the confinement length has a value $\alpha = 6.3 \pm 0.2$, independent of the wire diameter over the range 4−25 nm. At the low diameter limit of this study, i.e., $\bar{D}\sim$4 nm, which amounts to ∼8 lattice constants, first principles lattice dynamics studies can be carried out and bond polarizability calculations for the Raman scattering from the optical phonons of these wires could be made.[21] It would be interesting, indeed, to push the present experimental studies to diameters in the range 2−4 nm and to compare the experimental results with both the first-principal calculations/bond polarizability scattering and also the Raman line shape predicted by the phenomenological Richter model.

Acknowledgment. This work was supported by a grant from the NFS-NIRT program (Nanotechnology and Interdisciplinary Research Initiative), grant DMR-0304178. H.R.G. was supported by the NSF-UPenn-MRSEC, grant DMR00-79909.

References

(1) Zang, Y. F.; Tang, Y. H.; Wang, N.; Yu, D. P.; Lee, C. S.; Bello, I.; Lee, S. T. *Appl. Phys. Lett.* **1998**, *72*(15), 1835. Yu, D. P.; Bai, Z. G.; Ding, Y.; Hang, Q. L.; Zang, H. Z.; Wang, J. J.; Zou, H. Y.; Qian, W.; Xiong, G. C.; Zhou, H. T.; Feng, S. Q. *Appl. Phys. Lett.* **1998**, *72*(26), 3458. Zang, S. L.; Ding, W.; Yan, Y.; Qu, J.; Li, B.; Li, L. Y.; Yue, K. T.; Yu, D. P. *Appl. Phys. Lett.* **2002**, *81*, 4446.

(2) (a) Li, B.; Yu, D.; Zhang, S. L. *Phys. Rev. B* **1999**, *59*(3), 1645. (b) Hofmann, S.; Ducati, C.; Neill, R. J.; Piscanec, S.; Ferrari, A. C. *J. Appl. Phys.* **2003**, *94*, 6005. (c) Liu, J.; Niu, J.; Yang, D.; Yan, M.; Sha, J. *Physica E* **2004**, *23*, 221.

(3) Wang, R. P.; Zhou, G. W.; Liu, Y. L.; Pan, S. H.; Zhang, H. Z.; Yu, D. P.; Zhang, Z. *Phys. Rev. B* **2000**, *61*(24), 16827.

(4) Piscanec, S.; Ferrari, A. C.; Cantoro, M.; Hofmann, S.; Zapien, J. A.; Lifshift, Y.; Lee, S. T.; Robertson, J. *Mater. Sci. Eng. C−Bio.* **2003**, *23*(6−8), 931.

(5) Piscanec, S.; Cantoro, M.; Ferrari, A. C.; Zapien, J. A.; Lifshift, Y.; Lee, S. T.; Hofmann, S.; and Robertson, J. *Phys. Rev. B* **2003**, *68*, 241312(R).

(6) Gupta, R.; Xiong, Q.; Adu, C. K.; Kim, U. J.; Eklund, P. C. *Nano Lett.* **2003**, *3*(5), 627.

(7) Bhattacharyya, S.; Samui, S. *Appl. Phys. Lett.* **2004**, *84*(9), 1564.

(8) Richter, H.; Wang, Z. P.; Ley, Y. *Solid State Commun.* **1981**, *39*, 625.

(9) Adu, K. W.; Kim, U. J.; Gutierrez, H. R.; Eklund, P. C., to be published.

(10) Campbell, I. H.; Fauchet, P. M. *Solid State Commun.* **1986**, *58*, 739.

(11) Adu, K. W.; Gutierrez, H. R.; Kim, U. J.; Eklund, P. C., to be published.

(12) Xiong, Q.; Gupta, R.; W., A. K.; Dickey, E. C.; Lian, G. D.; Tham, D.; Fischer, J. E.; Eklund, P. C. *J. NanoSci. Technol.* **2003**, *3*(4), 335.

(13) Morales, A. M.; M., L. C. *Science* **1998**, *279*(5348), 208.

(14) Wu, Y.; Cui, Y.; Huynh, L.; Barrelet, C. J.; Bell, D. C.; Lieber, C. M. *Nano Lett.* **2004**, *4*(3), 433.

(15) Maeda, Y. *Phys. Rev. B* **1995**, *51*(3), 1658.

(16) Givargizov, E. I. *J. Cryst. Growth* **1975**, *31*, 20. Givargizov, E. I. *J. Cryst. Growth* **1973**, *20*, 217.

(17) Hart, T. R.; Aggarwal, R. L.; Lax, B. *Phys. Rev. B* **1970**, *1*(2), 638. Balkanski, M.; Wallis, R. F.; Haro, E. *Phys. Rev. B* **1981**, *28*(4), 1928.

(18) Mishra, P.; Jain, K. P. *Phys. Rev. B* **2000**, *62*, 14790.

(19) Nilsson, G.; Nelin, G. *Phys. Rev. B* **1972**, *6*, 3777.

(20) Thonhauser, T.; Mahan, G. D. *Phys. Rev. B* **2004**, *69*, 075213.

(21) Mahan, G. D. Work of this nature has been submitted for publication. Private communication.

NL0486259